Eur. Phys. J. A **30**, 65–70 (2006)
DOI 10.1140/epja/i2006-10106-9

THE EUROPEAN PHYSICAL JOURNAL A

Neck dynamics

M. Di Toro[1,a], A. Olmi[2], and R. Roy[3]

[1] Laboratori Nazionali del Sud INFN, Department of Physics and Astronomy, University of Catania, Via S. Sofia 62, I-95123, Italy
[2] INFN - Sezione di Firenze, Via G. Sansone 1, I-50019 Sesto Fiorentino, Italy
[3] Université Laval, Département de physique, de génie physique et d'optique, Cité universitaire, Québec, Qc, Canada, G1K 7P4

Received: 28 February 2006 /
Published online: 6 October 2006 –

Abstract. Intermediate-energy heavy-ion reactions produce a mid-rapidity region or neck, mostly in the semiperipheral collisions. Brief theory and experiment surveys are presented. General properties of the mid-rapidity zone are reviewed and discussed in the framework of reaction dynamics. Hierarchy effect, neutron enrichment, isospin diffusion are all new neck phenomena which are surveyed. The main neck observables are also examined, mainly in the context of the symmetry term of the nuclear equation of state.

PACS. 25.70.-z Low and intermediate energy heavy-ion reactions – 25.70.Lm Strongly damped collisions – 25.70.Mn Projectile and target fragmentation

1 Neck fragmentation in semiperipheral collisions at Fermi energies

1.1 Theory survey

The possibility of observation of new effects, beyond the deep-inelastic binary picture, in fragment formation for semicentral collisions with increasing energy was advanced on the basis of the reaction dynamics studied with transport models [1–3]. The presence of a time matching between the instability growth in the dilute overlap zone and the expansion-separation time scale suggested the observation of mean-field instabilities first at the level of anomalous widths in the mass/charge/... distributions of Projectile-Like or Target-Like (PLF/TLF) residues in binary events, then through a direct formation of fragments in the *neck region* [4,5]. It is clear that in the transport simulations stochastic terms should be consistently built in the kinetic equations in order to have a correct description of instability effects. Stochastic Mean-Field approaches have been introduced, reproducing the presently available data and having a large predictive power [6–9].

In conclusion, at the Fermi energies, we expect an interplay between binary and *neck fragmentation* events, where Intermediate Mass Fragments (IMF, in the range $3 \leq Z \leq 10$) are directly formed in the overlapping region, roughly at mid-rapidity in semicentral reactions. The competition between the two mechanisms is expected to be rather sensitive to the nuclear equation of state, in particular to its compressibility that will influence the interaction time as well as the density oscillation in the *neck region*. In the case of charge asymmetric colliding systems the poorly known stiffness of the symmetry term will also largely influence the reaction dynamics. An observable sensitive to the stiffness of the symmetry term can be just the relative yield of incomplete fusion *vs.* deep-inelastic in neck fragmentation events [10]. Moreover, for neutron-rich systems, in the asy-soft case we expect more interaction time available for charge equilibration. This means that even the binary events will show a sensitivity through a larger isospin diffusion. At variance, in the asy-stiff case the two final fragments will keep more memory of the initial conditions.

Systematic transport studies of isospin effects in the neck dynamics have been performed so far for collisions of Sn-Sn isotopes at 50 AMeV [6,7], Sn-Ni isotopes at 35 AMeV [8,9] and finally Fe-Fe and Ni-Ni, mass 58, at 30 and 47 AMeV [11].

1.2 Experimental survey

It is now quite well established that a large part of the reaction cross-section for dissipative collisions at Fermi energies goes through the *Neck Fragmentation* channel, with IMFs directly produced in the interacting zone in semiperipheral collisions on very short time scales. Before a clear *Neck Fragmentation* was proposed, out-of-equilibrium emission at mid-rapidity was observed for

[a] e-mail: ditoro@lns.infn.it

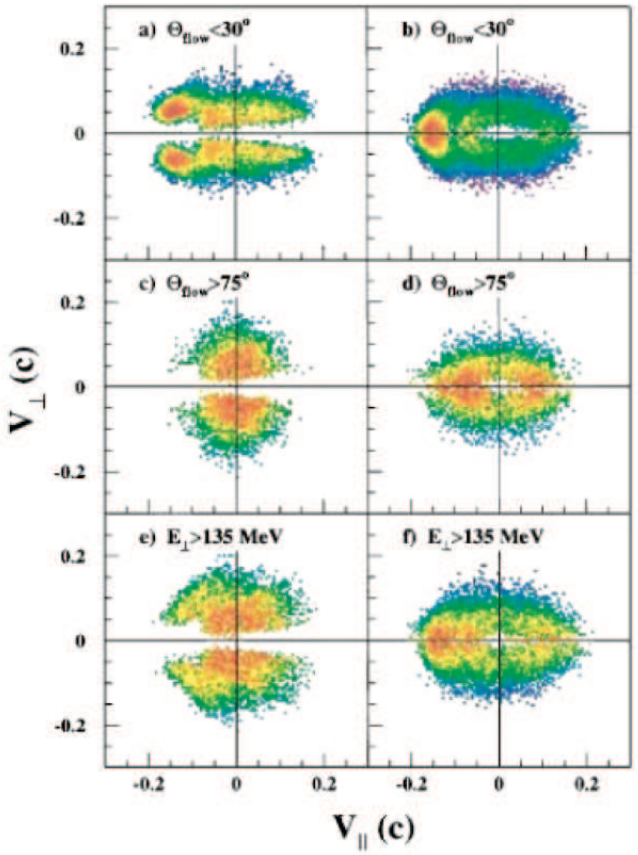

Fig. 1. Galilean-invariant perpendicular *vs.* parallel velocity in the c.m. frame for $Z = 3$ fragments. Parallel velocities are along the beam axis ((a),(c),(e)) and the main axis of the momentum tensor ((b),(d),(f)). Cuts on $\Theta_{flow} < 30°$ ((a),(b)), $\Theta_{flow} > 75°$; ((c),(d)), and on $E_\perp > 135\,\mathrm{MeV}$ which is the top 10% of the $E_\perp$ distribution: ((e),(f)) are made. The count yield is in a logarithmic scale. (From [24].)

IMFs and light charged particles [12–15]. From ternary fission, a non-statistical angular emission pattern was also observed for the IMFs [16–18]. We can expect different isospin effects for this new fragment formation mechanism since clusters are formed still in a dilute asymmetric matter but always in contact with the regions of the projectile-like and target-like remnants almost at normal densities.

A first evidence of this new dissipative mechanism was suggested at quite low energies, around 19 AMeV, in semi-central $^{100}\mathrm{Mo} + {}^{100}\mathrm{Mo}$, $^{120}\mathrm{Sn} + {}^{120}\mathrm{Sn}$ reactions [19,20]. A transition from binary, deep-inelastic, to ternary events was observed, with a dynamically formed fragment that influences the fission-like decay of the primary projectile-like PLF and target-like TLF partners. From the in-plane fragment angular distribution a decrease of scission-to-scission lifetimes with the mass asymmetry of the PLF or TLF "fission-fragments" down to $200\,\mathrm{fm}/c$ has been deduced. Similar conclusions were reached in [21,22]. Consistent with the dynamical scenario was the anisotropic azimuthal distribution of IMFs. In fact the IMF *alignment* with respect to the (PLF*) velocity direction has been one clear property of the "neck fragments" first noticed by Montoya *et al.* [23] for $^{129}\mathrm{Xe} + {}^{63,65}\mathrm{Cu}$ at 50 AMeV. As an example in the same context, fig. 1, from [24], displays an important neck component for $Z = 3$ particles in a much lighter system, $^{35}\mathrm{Cl} + {}^{12}\mathrm{C}$ at 43 AMeV. The flow angle and the total transverse energy are the observable used for impact parameter selection.

In peripheral collisions around 30 AMeV, the IMF production cross-section presents a maximum at mid-rapidity, but their experimental emission pattern cannot be reproduced without a sizable contribution of fragments emitted on a rather short time scale ($< 300\,\mathrm{fm}/c$) and almost at rest in the PLF or TLF reference frame [25]. Light charged particles also show a short time scale at mid-rapidity [26, 27]. With increasing bombarding energy, the mid-rapidity region of peripheral collisions becomes progressively depleted, while the IMFs are increasingly concentrated on Coulomb-like rings around the projectile and target rapidities [28]. However, their distribution on these rings is anisotropic, with a strong preference for emissions toward mid-rapidity. This behavior is particularly evident in the $^{197}\mathrm{Au} + {}^{197}\mathrm{Au}$ data of ref. [29].

The velocity of the projectile remnants and the distribution of mid-rapidity particles indicate that the mid-rapidity or neck emission mechanism represents an important effect in the excitation energy deposition [30]. Indeed, a recent comparison of the emissions from mid-rapidity with the evaporative emissions from the excited PLF shows that this mechanism has an important role in the overall balance of the reaction (both in terms of emitted mass or charge and energy) and that an important part of the dissipated energy is localized at mid-rapidity [31]. This suggests that a rather large energy density is stored in the contact region of the colliding nuclei and may also explain the well-established feature of an enhanced emission of mid-rapidity IMFs.

A rise and fall of the neck mechanism for mid-rapidity fragments with the centrality, with a maximum for intermediate impact parameters $b \simeq \frac{1}{2} b_{max}$, as observed in [32, 33], suggests the special physical conditions required. The size of the participant zone is of course important but it also appears that a good time matching between the time scales of the reaction and the neck instabilities is also needed, as suggested in refs. [1,4]. In fact a simultaneous presence, in non-central collisions, of different IMF production mechanisms at mid-rapidity was inferred in several experiments [34–44].

An accurate analysis of charge, parallel velocity, and angular distributions has been extended to high fragment multiplicities by Colin *et al.* [43]. They have noticed a "hierarchy effect": the ranking in charge induces on average a ranking in the velocity component along the beam, v_{par}, and in the angular distribution. This means that the heaviest IMF formed in the mid-rapidity region is the fastest and the most forward peaked, consistent with the formation and breakup of a neck structure or a strongly deformed quasiprojectile. A very precise and stimulating study of the time scales in neck fragmentation can be car-

ried out using the new 4π detectors with improved performances on mass resolution and thresholds for fragment measurements. Such kind of data are now appearing from the Chimera Collaboration [44].

We can immediately expect an important isospin dependence of the neck dynamics, from the presence of large density gradients and from the possibility of selecting various time scales for the fragment formation. The first evidences of isospin effects in neck fragmentation were suggested by Dempsey *et al.* [45] from semiperipheral collisions of the systems $^{124,136}\mathrm{Xe} + {}^{112,124}\mathrm{Sn}$ at 55 AMeV, where correlations between the average number of IMFs, N_{IMF}, and neutron and charged-particle multiplicities were measured. The variation of the relative yields of $^{6}\mathrm{He}/^{3,4}\mathrm{He}$, $^{6}\mathrm{He}/\mathrm{Li}$ with v_{par} for several Z_{PLF} gates shows that the fragments produced in the mid-rapidity region are more neutron rich than are the fragments emitted by the PLF. Enhanced *triton* production at mid-rapidity was considered in ref. [33], and more recently in [46], as an indication of a neutron neck enrichment.

Milazzo *et al.* [47–49] analyzed the IMF parallel velocity distribution for $^{58}\mathrm{Ni} + {}^{58}\mathrm{Ni}$ semiperipheral collisions at 30 AMeV. The two-bump structure for IMFs with $5 \leq Z \leq 12$, located around the center-of-mass velocity and close to the projectile (PLF^*) source, respectively, was explained assuming the simultaneous presence of two production mechanisms: the statistical disassembly of an equilibrated PLF^* and the dynamical fragmentation of the participant region. The separation of the two contributions allows for several interesting conclusions. The average elemental event multiplicity $N(Z)$ exhibits a different trend for the two processes: in particular, the fragments with $5 \leq Z \leq 11$ are more copiously produced at the mid-rapidity region. This experiment has a particular importance since isospin effects were clearly observed, *in spite of the very low initial asymmetry*. The measured isotopic content of the fragments is clearly different in the two mechanisms. The experimental heavy-isotope/light-isotope yield ratios, $^{14}\mathrm{C}/^{12}\mathrm{C}$, $^{12}\mathrm{B}/^{10}\mathrm{B}$, $^{10}\mathrm{Be}/^{7}\mathrm{Be}$, $^{8}\mathrm{Li}/^{6}\mathrm{Li}$, show a systematic decreasing trend as a function of parallel velocity from c.m. to PLF values.

All these results indicate a neutron enrichment of the neck region, *even when initially the system N/Z is close to unity*. The same reactions have been recently studied at the Cyclotron Institute of Texas A&M at various beam energies with measurements of the correlations of fragment charge/mass *vs.* dynamical observables (emission angles and velocities) [50,51].

Plagnol *et al.* [52] have examined, for the system Xe + Sn between 25 and 50 AMeV, the competition between mid-rapidity dynamical emission and equilibrium evaporation as well as its evolution with incident energy. The onset of the neck emission takes place around 25 AMeV and rises with the energy while the evaporative part remains quite invariant for a selected centrality. Neck matter is found to be more charge asymmetric: more neutron-rich isotopes are favored at mid-rapidity in comparison to evaporation. Evidence of a neck-like structure and its neutron enrichment has been seen even in collisions

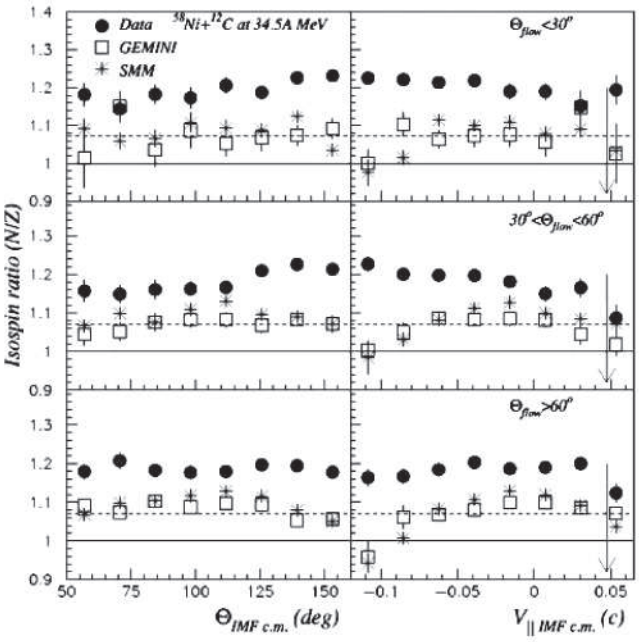

Fig. 2. Average isospin ratios (N/Z) for well-identified IMFs with $Z = 3$ or 4 as a function of the emission angle in the center-of-mass reference frame (left) and the center-of-mass particle velocity parallel to the beam axis (right) for the reaction $^{58}\mathrm{Ni} + {}^{12}\mathrm{C}$ at 34.5 AMeV (full dots). Cuts are made on $\Theta_{flow} < 30°$ (top), $30° < \Theta_{flow} < 60°$ (middle), and $\Theta_{flow} > 60°$ (bottom). Open boxes represent filtered GEMINI simulations and stars are results from filtered SMM simulations. Error bars are the statistical errors for a given angle or velocity bin. When no error bar is present, the error is smaller than the size of the symbol. The dotted lines show the isospin ratio for $^{58}\mathrm{Ni}$ (1.07) and the full line for $^{12}\mathrm{C}$ (1.00). The arrow shows the velocity of the $^{58}\mathrm{Ni}$ projectile in the center-of-mass frame for the $^{58}\mathrm{Ni} + {}^{12}\mathrm{C}$ reaction. (From [53].)

with a rather light symmetric target, $^{58}\mathrm{Ni} + {}^{12}\mathrm{C}$, $^{24}\mathrm{Mg}$, at 34.5 AMeV [53]. The average N/Z ratio for isotopes with $Z = 3, 4$ exhibits a clear increase from the PLF to the mid-rapidity zone. Figure 2 from [53] shows part of those measurements. Also, a combined analysis of the $^{58}\mathrm{Ni} + {}^{58}\mathrm{Ni}$ and $^{36}\mathrm{Ar} + {}^{58}\mathrm{Ni}$ systems around 50 AMeV has evidenced an asymmetric migration of neutrons and protons between the quasiprojectile and the mid-rapidity region [54]. Time sequence emission is another way to probe the neck rupture processes and to characterize the fragments [55].

That indicates the need of new, possibly more exclusive, data. The reasons for a preponderance of neutron-rich isotopes emitted from the neck region are a matter of debate. Possible explanations being, apart the density dependence of symmetry energy [56], also a fast light cluster production, especially of α-particles, which promptly leads to an amplification of neutron excess in the participant matter [57]. For completeness, we have to mention that different analyses even give conflicting results on the neutron enrichment of the clusters produced at mid-rapidity [58,59]. This shows that the reaction dynamics

is in general very complicated, and there could even be different isospin effects in competition.

2 Isospin diffusion

The isospin equilibration appears of large interest also for more peripheral collisions, where we have shorter interaction times, less overlap and a competition between binary and neck fragmentation processes. The specific feature at Fermi energies is that the interaction times are close to the specific time scales for isospin transport allowing a more detailed investigation of isospin diffusion and equilibration in reactions between nuclei with different N/Z asymmetries. The low-density neck formation and the pre-equilibrium emission are adding essential differences with respect to what is happening in the lower-energy regime. Tsang *et al.* [60] have probed the isospin diffusion mechanism for the systems $^{124}\mathrm{Sn} + {}^{112}\mathrm{Sn}$ at $E = 50\,\mathrm{AMeV}$ in a peripheral impact parameter range $b/b_{max} > 0.8$, observing the isoscaling features of the light isotopes $Z = 3$–8 emitted around the projectile rapidity. An incomplete equilibration has been deduced. The value of the isoscaling parameter $\alpha = 0.42 \pm 0.02$ for $^{124}\mathrm{Sn} + {}^{112}\mathrm{Sn}$ differs substantially from $\alpha = 0.16 \pm 0.02$ for $^{112}\mathrm{Sn} + {}^{124}\mathrm{Sn}$. The isospin imbalance ratio [61], defined as

$$R_i(x) = \frac{2x - x^{124+124} - x^{112+112}}{x^{124+124} - x^{112+112}} \qquad (1)$$

($i = P, T$ refers to the projectile/target rapidity measurement, and x is an isospin-dependent observable, here the isoscaling α parameter) was estimated to be around $R_P(\alpha) = 0.5$ (*vs.* $R_P(\alpha) = 0.0$ in full equilibration). This quantity can be sensitive to the density dependence of symmetry energy term since the isospin transfer takes place through the lower-density neck region.

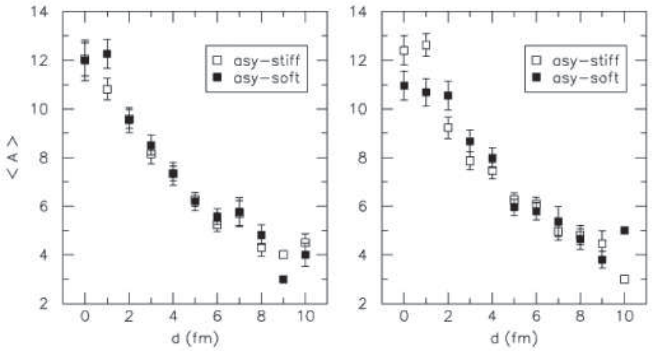

Fig. 3. Average IMF mass as a function of the distance from the PLF-TLF axis at the freeze-out time for 47 AMeV, for collisions at a reduced impact parameter of 0.5. Left panel: Fe + Fe. Right panel: Ni + Ni. Empty squares: asy-soft symmetry term. Full squares: asy-stiff. (From [11].)

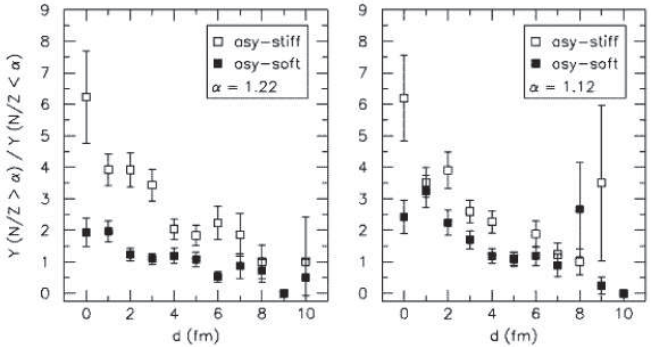

Fig. 4. Ratio of the IMF yields, with N/Z larger and smaller than the value α obtained just after pre-equilibrium emission, as a function of the distance from the PLF-TLF axis at the freeze-out time for 47 AMeV, for collisions at a reduced impact parameter of 0.5. Left panel: Fe + Fe. Right panel: Ni + Ni. Empty squares: asy-stiff symmetry term. Full squares: asy-soft. (From [11].)

3 Neck observables

– Properties of neck fragments, mid-rapidity IMF produced in semicentral collisions: correlations between N/Z, *alignment* and size.
The alignment between PLF-IMF and PLF-TLF directions represents a very convincing evidence of the dynamical origin of the mid-rapidity fragments produced on short time scales [8]. The form of the Φ_{plane} distributions (centroid and width) can give a direct information on the fragmentation mechanism [19,20, 62]. Recent calculations confirm a general feature, predicted for that rupture mechanism: the light fragments are emitted first, as displayed in fig. 3.
– Time scale measurements.
The estimation of time scales for fragment formation from velocity correlations appears to be a very exciting possibility [25,44,63]. With a good event-by-event detection of the projectile(target) residues we can measure the violations of the Viola systematics for the TLF-IMF and PLF-IMF systems which tell us how much the IMFs are uncorrelated to the *spectator* remnants [64].
With appropriate cuts in the velocity correlation plots we can follow the properties of clusters produced from sources with a "controlled" different degree of equilibration. We can figure out a continuous transition from fast-produced fragments via neck instabilities to clusters formed in a dynamical fission of the projectile(target) residues up to the evaporated ones (statistical fission). Along this line it would be even possible to disentangle the effects of volume and shape instabilities. The isospin dynamics will look different in the various scenarios and rather dependent on the symmetry term of the EOS.
– Isospin dynamics.
Isospin effects on the reaction dynamics and *Isospin Migration*: an interesting neutron enrichment of the overlap ("neck") region is expected, due to the neutron migration from higher (spectator) to lower (neck)

density regions. This effect is also nicely connected to the slope of the symmetry energy. Neutron and/or light isobar measurements in different rapidity regions appear important. Moreover, in moving from mid- to "spectator" rapidities, an increasing hierarchy in the mass and N/Z of the fragments is expected [11]. Some experimental evidences are in ref. [43]. An interesting related observable is the corresponding angular correlation due to the driving force of the projectile(target)-like partners [11].

– Isospin diffusion.
With measurements of charge equilibration in the "spectator" region in semicentral collisions, we can get the *Imbalance Ratios* for different isospin properties. It is a test of the interplay between concentration and density gradients in the isospin dynamics [9,65,66]. For the reasons noted before we expect to see a clear difference in the isospin diffusion between binary (deep-inelastic like) and neck fragmentation events. Moreover, in the mid-rapidity emission, there is a clear neutron enrichment predicted [11] for neutron-rich and neutron-poor systems (see fig. 4, from [11]).
– "Pre-equilibrium" emissions.
As already noted, the isospin content of the fast particle emission can largely influence the subsequent reaction dynamics, in particular, the isospin transport properties (charge equilibration, isospin diffusion). We can reach the paradox of a detection of isospin dynamics effects in charge symmetric systems.
Finally, the simultaneous measurements of properties of fast nucleon emissions and of the neck dynamics can even shed light on the very controversial problem of the isospin momentum dependence [9,66].

We stress the richness of the phenomenology and nice opportunities of getting several cross-checks from completely different experiments. Apart from the interest of this new dissipative mechanism and the amazing possibility of studying properties of fragments produced on an almost continuous range of time scales, we remark the expected dependence on the isovector part of the nuclear EOS. From transport simulations we presently get some indications of "asy-stiff" behaviors, *i.e.* increasing repulsive density dependence of the symmetry term, but not more fundamental details. Moreover, all the available data are obtained with stable beams, *i.e.* within low asymmetries.

References

1. A. Bonasera, G.F. Bertsch, E.N. El-Sayed, Phys. Lett. B **141**, 9 (1984).
2. M. Colonna, N. Colonna, A. Bonasera, M. Di Toro, Nucl. Phys. A **541**, 295 (1992).
3. L.G. Sobotka, Phys. Rev. C **50**, 1272R (1994).
4. M. Colonna, M. Di Toro, A. Guarnera, Nucl. Phys. A **589**, 160 (1995).
5. M. Di Toro *et al.*, Progr. Part. Nucl. Phys. **42**, 125 (1999).
6. M. Di Toro *et al.*, Nucl. Phys. A **681**, 426c (2001).
7. V. Baran, M. Colonna, V. Greco, M. Di Toro, M. Zielinska-Pfabé, H.H. Wolter, Nucl. Phys. A **703**, 603 (2002).
8. V. Baran, M. Colonna, M. Di Toro, Nucl. Phys. A **730**, 329 (2004).
9. V. Baran, M. Colonna, V. Greco, M. Di Toro, Phys. Rep. **410**, 335 (2005).
10. M. Colonna, M. Di Toro, G. Fabbri, S. Maccarone, Phys. Rev. C **57**, 1410 (1998).
11. R. Lionti, V. Baran, M. Colonna, M. Di Toro, Phys. Lett. B **625**, 33 (2005).
12. L. Stuttgé *et al.*, Nucl. Phys. A **539**, 511 (1992).
13. R. Wada *et al.*, Nucl. Phys. A **548**, 471 (1992).
14. D.E. Fields *et al.*, Phys. Rev. Lett. **69**, 3713 (1992).
15. J.E. Sauvestre *et al.*, Phys. Lett. B **335**, 300 (1994).
16. J. Boger *et al.*, Phys. Rev. C **41**, 801 (1990).
17. S.L. Chen *et al.*, Phys. Rev. C **54**, R2114 (1996).
18. R. Yanez *et al.*, Phys. Rev. Lett. **82**, 3585 (1999).
19. G. Casini *et al.*, Phys. Rev. Lett. **71**, 2567 (1993).
20. A.A. Stefanini *et al.*, Z. Phys. A **351**, 167 (1995).
21. J. Tõke *et al.*, Phys. Rev. Lett. **75**, 2920 (1995).
22. J.F. Lecolley *et al.*, Phys. Lett. B **354**, 202 (1995).
23. C.P. Montoya *et al.*, Phys. Rev. Lett. **73**, 3070 (1994).
24. L. Beaulieu *et al.*, Phys. Rev. Lett. **77**, 462 (1996).
25. S. Piantelli *et al.*, Phys. Rev. Lett. **88**, 052701 (2002).
26. P. Pawlowski *et al.*, Eur. Phys. J. A **9**, 371 (2000).
27. D. Doré *et al.*, Phys. Rev. C **63**, 034612 (2001).
28. W.G. Lynch, Nucl. Phys. A **583**, 471c (1995).
29. J. Łukasik *et al.*, Phys. Lett. B **566**, 76 (2003).
30. Y. Larochelle *et al.*, Phys. Rev. C **59**, R565 (1999).
31. A. Mangiarotti *et al.*, Phys. Rev. Lett. **93**, 232701 (2004).
32. J. Péter *et al.*, Nucl. Phys. A **593**, 95 (1995).
33. J. Łukasik *et al.*, Phys. Rev. C **55**, 1906 (1997).
34. J. Tõke *et al.*, Nucl. Phys. A **583**, 519c (1995).
35. J. Tõke *et al.*, Phys. Rev. Lett. **77**, 3514 (1996).
36. Y. Larochelle *et al.*, Phys. Rev. C **55**, 1869 (1997).
37. P. Pawlowski *et al.*, Phys. Rev. C **57**, 1771 (1998).
38. T. Lefort *et al.*, Nucl. Phys. A **662**, 397 (2000); D. Doré *et al.*, Phys. Lett. B **491**, 15 (2000).
39. F. Bocage *et al.*, Nucl. Phys. A **676**, 391 (2000).
40. B. Grabez, Phys. Rev. C **64**, 057601 (2001).
41. L. Gingras *et al.*, Phys. Rev. C **65**, 061604 (2002).
42. B. Davin *et al.*, Phys. Rev. C **65**, 064614 (2002).
43. J. Colin *et al.*, Phys. Rev. C **67**, 064603 (2003).
44. A. Pagano *et al.*, Nucl. Phys. A **734**, 504c (2004).
45. J.F. Dempsey *et al.*, Phys. Rev. C **54**, 1710 (1996).
46. G. Poggi, Nucl. Phys. A **685**, 296c (2001).
47. P.M. Milazzo *et al.*, Phys. Lett. B **509**, 204 (2001).
48. P.M. Milazzo *et al.*, Nucl. Phys. A **703**, 466 (2002).
49. P.M. Milazzo *et al.*, Nucl. Phys. A **756**, 39 (2005).
50. D.V. Shetty *et al.*, Phys. Rev. C **68**, 021602(R) (2003).
51. D.V. Shetty *et al.*, Phys. Rev. C **70**, 011601(R) (2004).
52. E. Plagnol *et al.*, Phys. Rev. C **61**, 014606 (2000).
53. Y. Larochelle *et al.*, Phys. Rev. C **62**, 051602(R) (2000).
54. D. Thériault *et al.*, Phys. Rev. C **71**, 014610 (2005).
55. Chimera Collaboration (E. De Filippo *et al.*), Phys. Rev. C **71**, 044602 (2005).
56. S. Hudan *et al.*, Phys. Rev. C **71**, 054604 (2005).
57. L.G. Sobotka *et al.*, Phys. Rev. C **55**, 2109 (1997).
58. L.G. Sobotka *et al.*, Phys. Rev. C **62**, 031603(R) (2000).
59. H. Xu *et al.*, Phys. Rev. C **65**, 061602(R) (2002).
60. M.B. Tsang *et al.*, Phys. Rev. Lett. **92**, 062701 (2004).
61. F. Rami *et al.*, Phys. Rev. Lett. **84**, 1120 (2000).
62. Chimera Collaboration (E. De Filippo, A. Pagano, E. Piasecki *et al.*), Phys. Rev. C **71**, 064604 (2005).

63. Chimera Collaboration (J. Wilczyński *et al.*), Int. J. Mod. Phys. E **14**, 353 (2005); Chimera Collaboration (E. De Filippo *et al.*), Phys. Rev. C **71**, 044602 (2005).
64. It has been proposed to call the Viola-violation-correlation plot as *Wilczyński-2 Plot*. Indeed this correlation, very important to rule out a statistical fission scenario for fragments produced at mid-rapidity, nicely emerged during hot discussions of one of us (M.D.T.) with J. Wilczyński at the LNS-INFN, Catania. In fact this correlation represents also a *chronometer* of the fragment formation mechanism. In this sense it is the nice Fermi energy complement of the famous *Wilczyński Plot* which gives the time scales in Deep-Inelastic Collisions.
65. V. Baran, M. Colonna, M. Di Toro, M. Zielinska-Pfabé, H.H. Wolter, Phys. Rev. C **72**, 064620 (2005).
66. L.-W. Chen, C.M. Ko, B.-A. Li, Phys. Rev. Lett. **94**, 032701 (2005).